

ChemSusChem

Supporting Information

Butane Dry Reforming Catalyzed by Cobalt Oxide Supported on Ti₂AlC MAX Phase

Maria Ronda-Lloret, Vijaykumar S. Marakatti, Willem G. Sloof, Juan José Delgado, Antonio Sepúlveda-Escribano, Enrique V. Ramos-Fernandez, Gadi Rothenberg, and N. Raveendran Shiju*This publication is part of a Special Issue entitled "Green Carbon Science: CO₂ Capture and Conversion". Please visit the issue at .© 2020 The Authors. Published by Wiley-VCH GmbH. This is an open access article under the terms of the Creative Commons Attribution Non-Commercial License, which permits use, distribution and reproduction in any medium, provided the original work is properly cited and is not used for commercial purposes.

SUPPORTING INFORMATION

This document contains supplementary data on the characterization of the catalysts (XRD patterns, STEM-HAADF images, nitrogen adsorption-desorption isotherms, temperature programmed reduction profiles, thermogravimetric analysis and XPS data). The results of the control catalytic tests, as well as the selectivity and carbon balance plots of $\text{Co}_3\text{O}_4/\text{Ti}_2\text{AlC}$, $\text{Co}_3\text{O}_4/\text{Al}_2\text{O}_3$ and $\text{Co}_3\text{O}_4/\text{TiO}_2$ are also included.

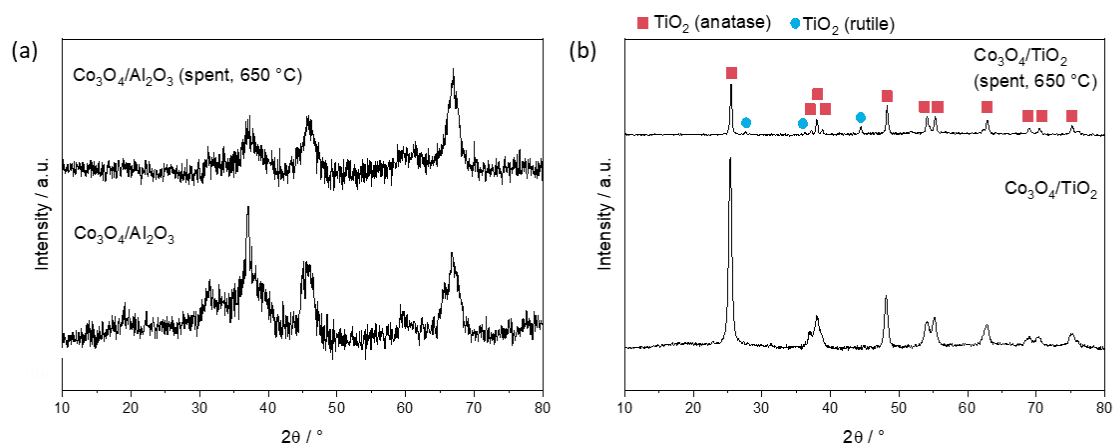


Figure S1. XRD patterns of (a) as-prepared $\text{Co}_3\text{O}_4/\text{Al}_2\text{O}_3$ and $\text{Co}_3\text{O}_4/\text{Al}_2\text{O}_3$ after stability test (spent, 650 °C), (b) as-prepared $\text{Co}_3\text{O}_4/\text{TiO}_2$ and $\text{Co}_3\text{O}_4/\text{TiO}_2$ after stability test (spent, 650 °C).

SUPPORTING INFORMATION

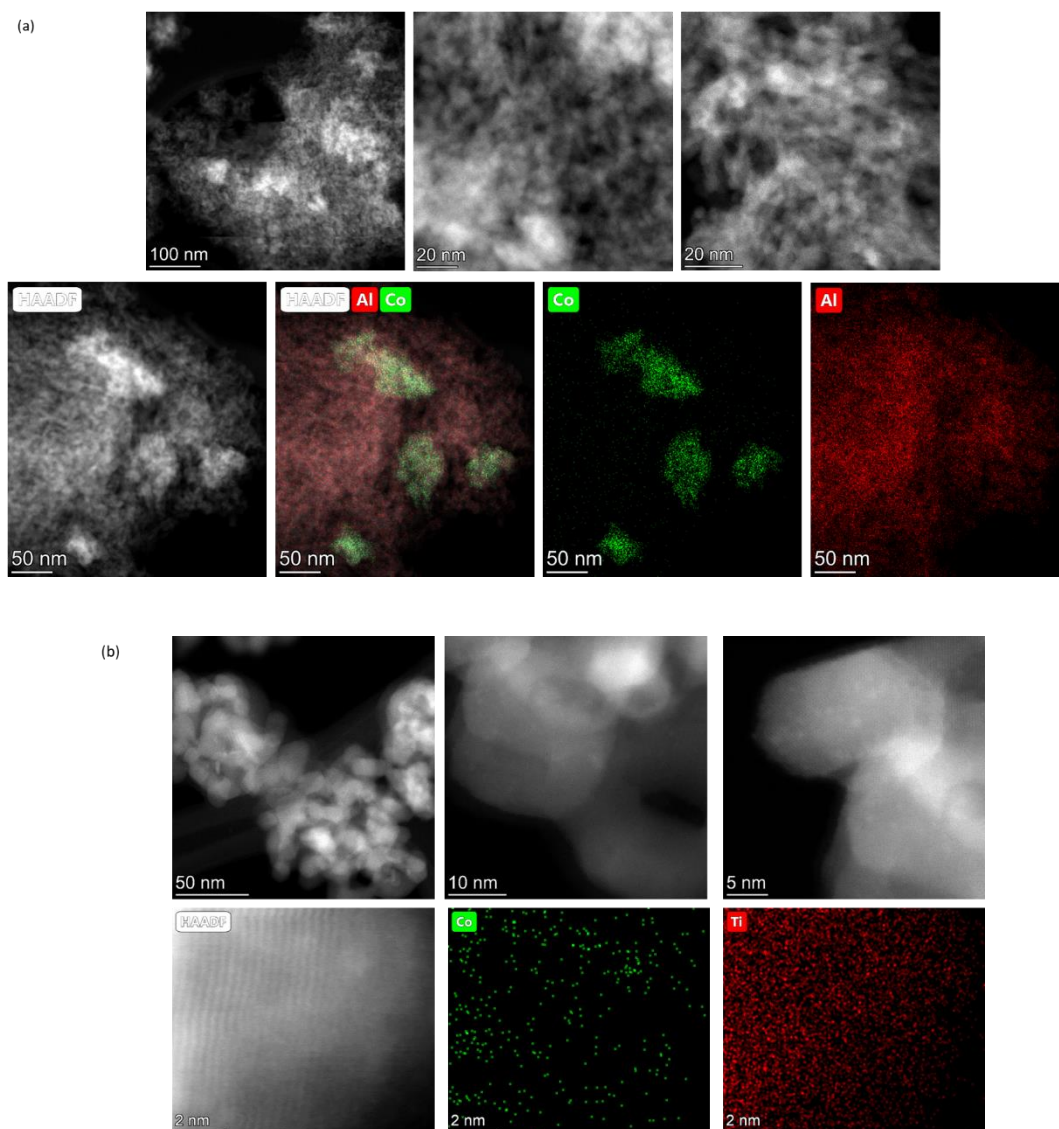


Figure S2. HAADF-STEM images of (a) $\text{Co}_3\text{O}_4/\text{Al}_2\text{O}_3$ and (b) $\text{Co}_3\text{O}_4/\text{TiO}_2$ catalysts, including Co, Al and Ti elemental distribution maps.

SUPPORTING INFORMATION

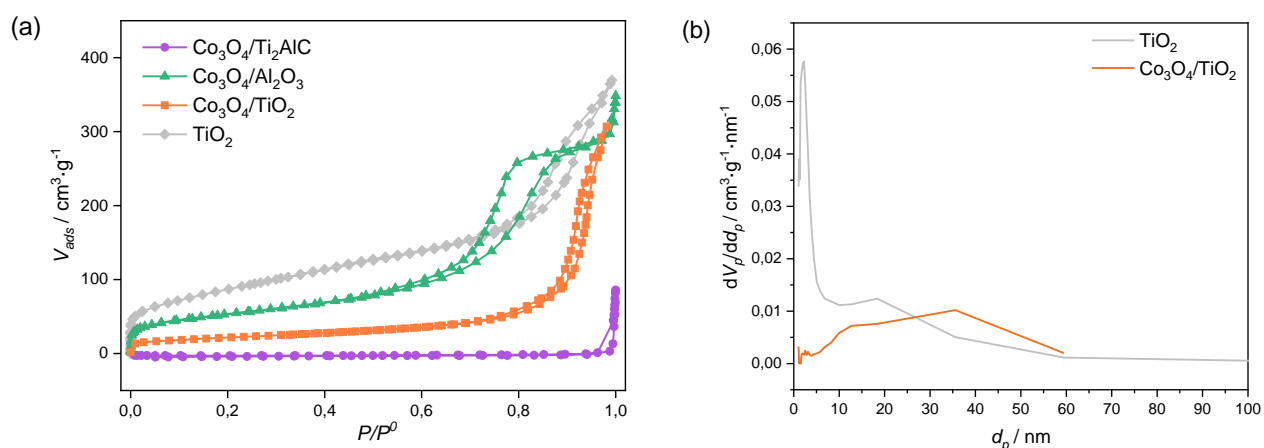


Figure S3. a) Nitrogen adsorption-desorption isotherms of the studied catalysts. b) BJH pore size distribution of TiO₂ and Co₃O₄/TiO₂ materials.

Table S1. BET surface area (S_{BET}), total pore volume (V_t), micropore volume (V_0), mesopore volume (V_{meso}) and average pore diameter values of the studied catalysts.

Catalyst	$S_{BET} / \text{m}^2 \cdot \text{g}^{-1}$	$V_t / \text{cm}^3 \cdot \text{g}^{-1}$	$V_0 / \text{cm}^3 \cdot \text{g}^{-1}$	$V_{meso} / \text{cm}^3 \cdot \text{g}^{-1}$	Average pore diameter (nm)
Co ₃ O ₄ /Ti ₂ AlC ^a	-	-	-	-	-
Co ₃ O ₄ /Al ₂ O ₃	187	0.43	0.05	0.38	9
Co ₃ O ₄ /TiO ₂	76	0.48	0.06	0.42	22
TiO ₂	316	0.57	0.10	0.47	6

^a Co₃O₄/Ti₂AlC values are not reported because this sample is not accessible for N₂.

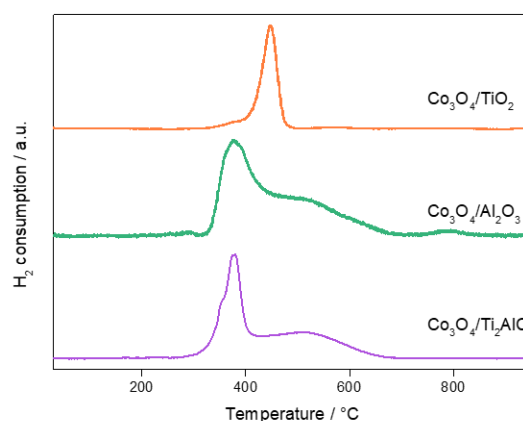


Figure S4. Temperature programmed reduction profiles of Co₃O₄/Ti₂AlC, Co₃O₄/Al₂O₃ and Co₃O₄/TiO₂ catalysts, under a flow of 5% H₂/N₂ mixture.

SUPPORTING INFORMATION

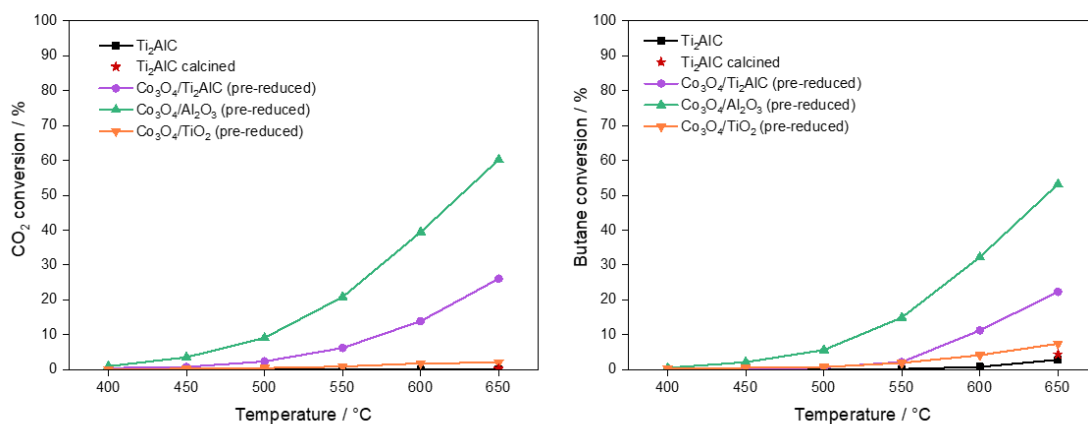


Figure S5. CO₂ and butane conversion during temperature screening of Ti₂AlC, Ti₂AlC calcined at 450 °C and the pre-reduced 5 wt% catalysts. Reduction conditions: 650 °C, 1h, 70% H₂ and 30% Ar mixture, 10 mL·min⁻¹. Reaction conditions: 100 mg of catalyst, CO₂:C₄H₁₀ = 4:1, total flow 20 mL·min⁻¹, atmospheric pressure.

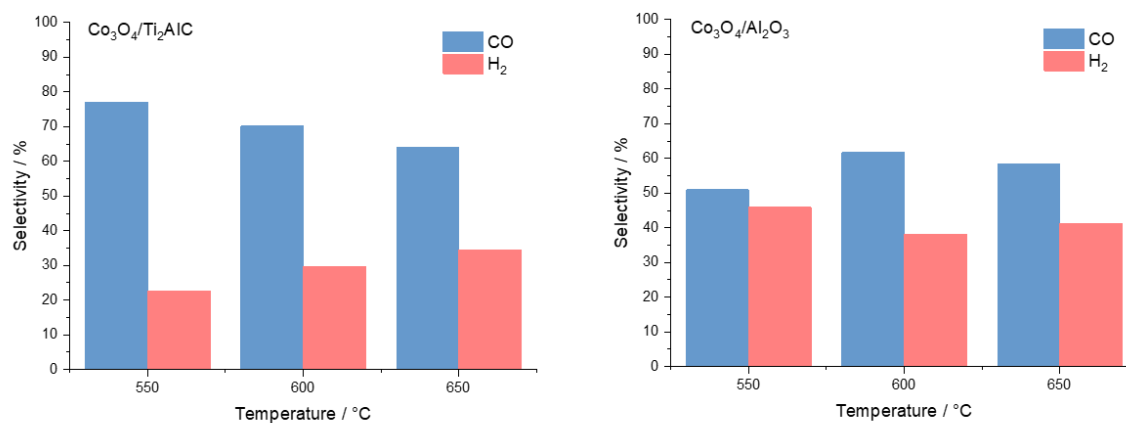


Figure S6. Selectivity during temperature screening of 5 wt.% Co₃O₄/Ti₂AlC and Co₃O₄/Al₂O₃ catalysts. Reaction conditions: 100 mg of catalyst, CO₂:C₄H₁₀ = 4:1, total flow 20 mL·min⁻¹, atmospheric pressure.

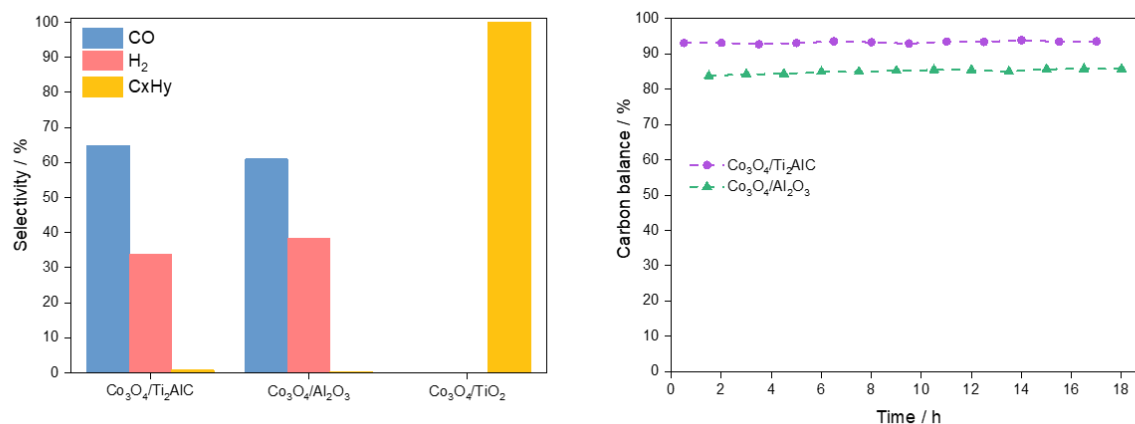


Figure S7. Selectivity (at 12 h) and carbon balance during stability test of 5 wt% catalysts. Reaction conditions: 100 mg of catalyst, CO₂:C₄H₁₀ = 4:1, total flow 20 mL·min⁻¹, atmospheric pressure.

SUPPORTING INFORMATION

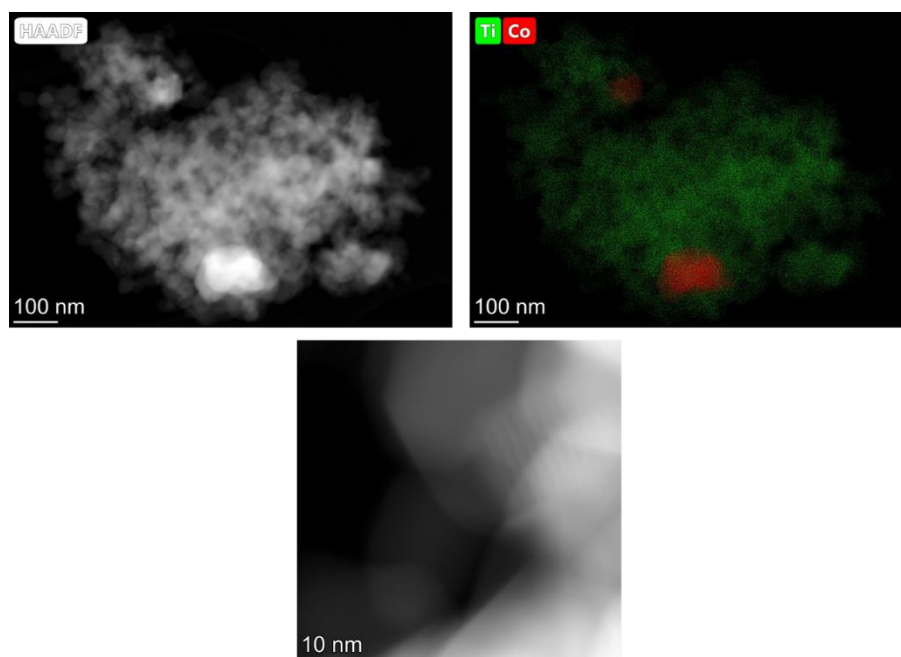


Figure S8. HAADF-STEM images of $\text{Co}_3\text{O}_4/\text{TiO}_2$ catalyst after stability test at $650\text{ }^\circ\text{C}$, which show the agglomeration of Co_3O_4 particles on the support. The HRTEM image shows the absence of small particles as in the fresh catalyst.

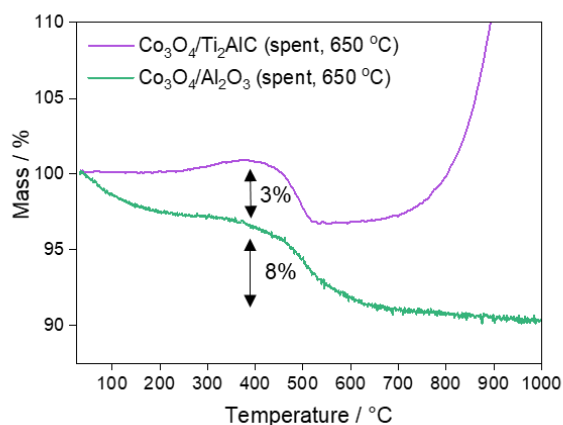


Figure S9. Thermogravimetric analysis of the samples after stability test at $650\text{ }^\circ\text{C}$ for 18 hours. Coke combustion takes place at temperatures between 300 and $600\text{ }^\circ\text{C}$. $\text{Co}_3\text{O}_4/\text{Ti}_2\text{AlC}$ catalyst experiences mass gain corresponding to the oxidation of Ti_2AlC to TiO_2 and Al_2O_3 during the measurement.

Table S2. NH_3 adsorption-desorption measurements of $\text{Co}_3\text{O}_4/\text{Ti}_2\text{AlC}$ and $\text{Co}_3\text{O}_4/\text{Al}_2\text{O}_3$ catalysts.

Catalyst	NH_3 desorption / $\mu\text{mol NH}_3 \cdot \text{g catalyst}^{-1}$
$\text{Co}_3\text{O}_4/\text{Ti}_2\text{AlC}$	11
$\text{Co}_3\text{O}_4/\text{Al}_2\text{O}_3$	128

SUPPORTING INFORMATION

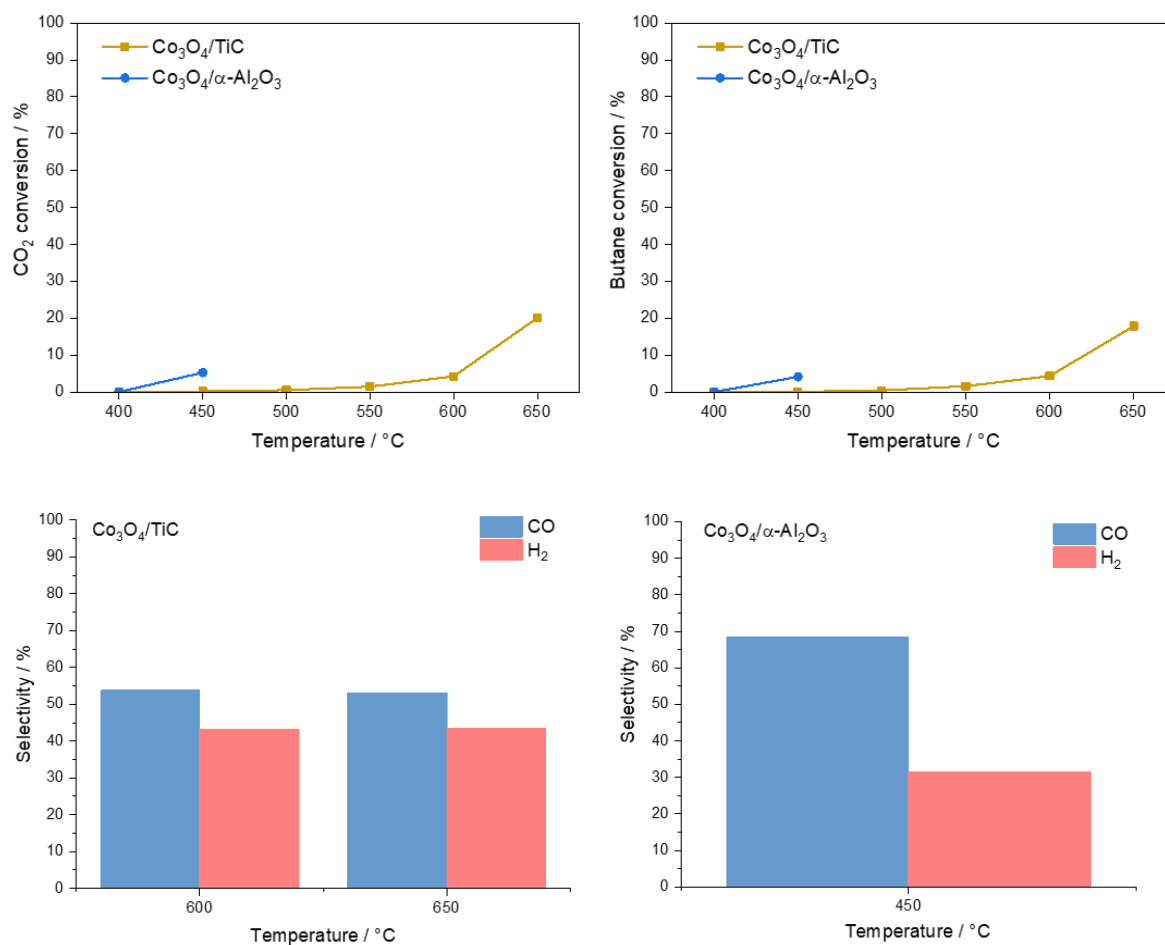


Figure S10. CO₂ and butane conversion and selectivity during temperature screening of Co₃O₄/TiC and Co₃O₄/α-Al₂O₃. Reaction conditions: 100 mg of catalyst, CO₂:C₄H₁₀ = 4:1, total flow 20 mL·min⁻¹, atmospheric pressure.

SUPPORTING INFORMATION

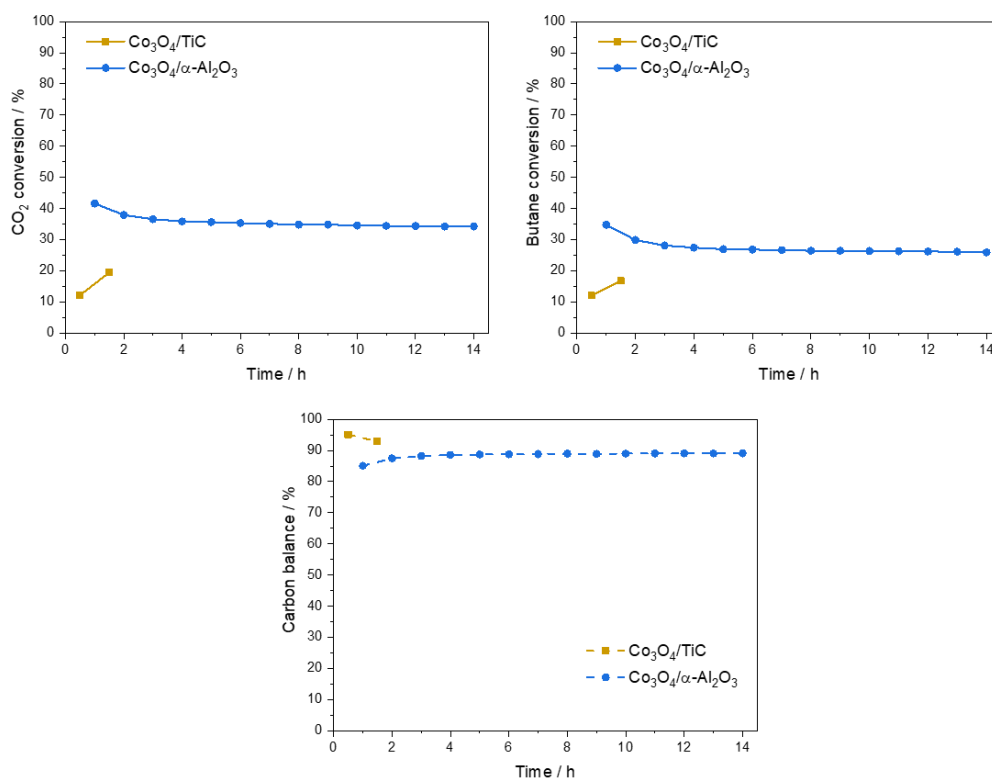


Figure S11. Conversion and carbon balance values during stability test of $\text{Co}_3\text{O}_4/\text{TiC}$ and $\text{Co}_3\text{O}_4/\alpha\text{-Al}_2\text{O}_3$. Reaction conditions: 650 °C, 100 mg of catalyst, $\text{CO}_2:\text{C}_4\text{H}_{10} = 4:1$, total flow $20 \text{ mL}\cdot\text{min}^{-1}$, atmospheric pressure.

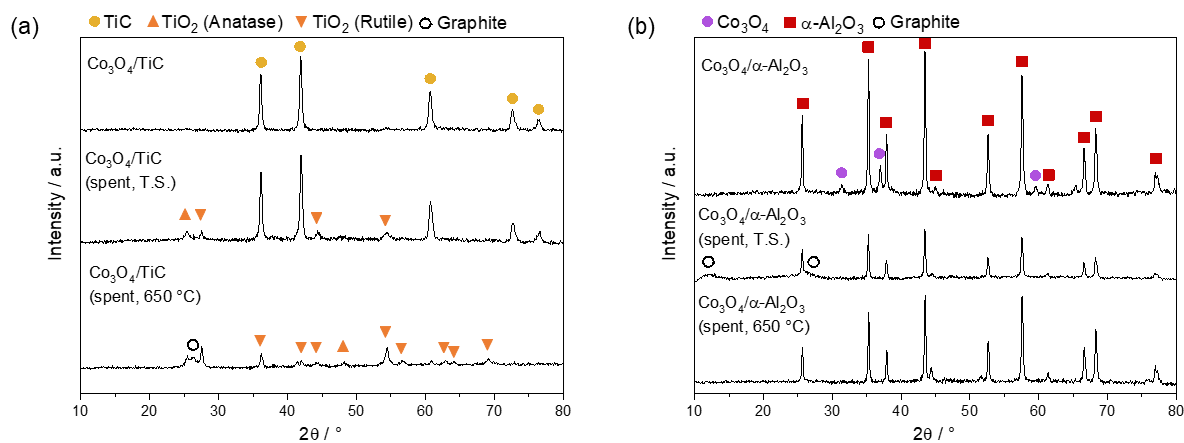
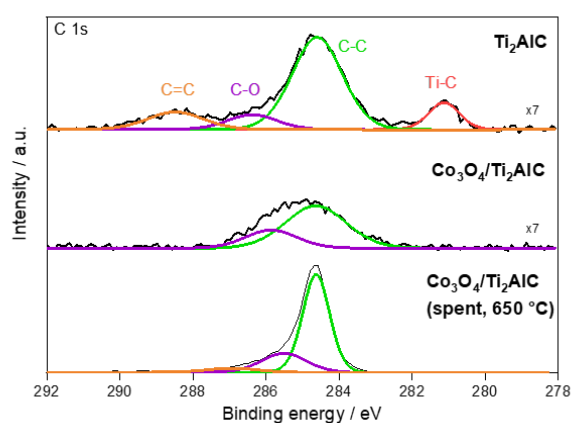
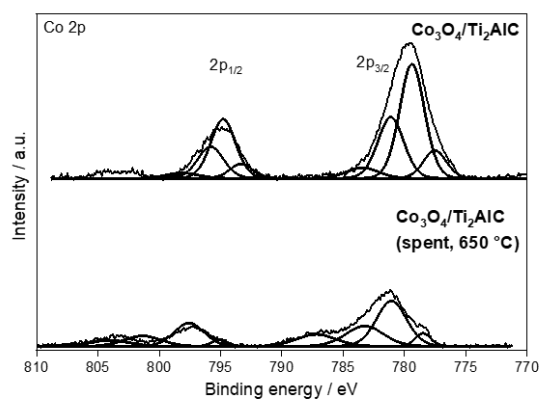


Figure S12. XRD patterns of $\text{Co}_3\text{O}_4/\text{TiC}$ and $\text{Co}_3\text{O}_4/\alpha\text{-Al}_2\text{O}_3$ as-prepared, after temperature screening tests (spent, T.S.) and after stability tests (spent, 650 °C).

SUPPORTING INFORMATION

Table S3. Atomic percentage of Co, Ti, Al, C and O on the surface of the catalysts and the intensity ratios between cobalt and support particles, obtained from XPS analysis.

Catalyst	Atom fraction (%) on the surface					$I_{\text{Co}}/I_{\text{Al}}$ ratio	$I_{\text{Co}}/I_{\text{Ti}}$ ratio
	Co	Ti	Al	C	O		
$\text{Co}_3\text{O}_4/\text{Ti}_2\text{AlC}$	12.86	6.39	9.08	15.09	56.58	1.42	2.01
$\text{Co}_3\text{O}_4/\text{Ti}_2\text{AlC}$ (spent, 650 °C)	3.62	3.64	6.93	59.91	25.9	0.52	0.99
$\text{Co}_3\text{O}_4/\text{TiO}_2$	2.33	16.37	-	27.45	54.26	-	0.14
$\text{Co}_3\text{O}_4/\text{Al}_2\text{O}_3$	0.55	-	25.24	23.77	50.44	0.02	-

**Figure S13.** C 1s photoelectron spectra of Ti_2AlC , fresh $\text{Co}_3\text{O}_4/\text{Ti}_2\text{AlC}$ and $\text{Co}_3\text{O}_4/\text{Ti}_2\text{AlC}$ after stability test (spent, 650 °C).**Figure S14.** Co 2p photoelectron spectra of fresh $\text{Co}_3\text{O}_4/\text{Ti}_2\text{AlC}$ and $\text{Co}_3\text{O}_4/\text{Ti}_2\text{AlC}$ after stability test (spent, 650 °C).

SUPPORTING INFORMATION

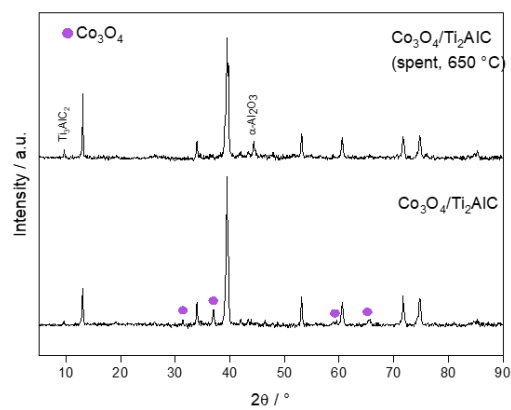


Figure S15. Comparison of the XRD patterns of as-prepared Co_3O_4/Ti_2AlC and Co_3O_4/Ti_2AlC catalyst after stability test (spent, 650 °C).

SUPPORTING INFORMATION

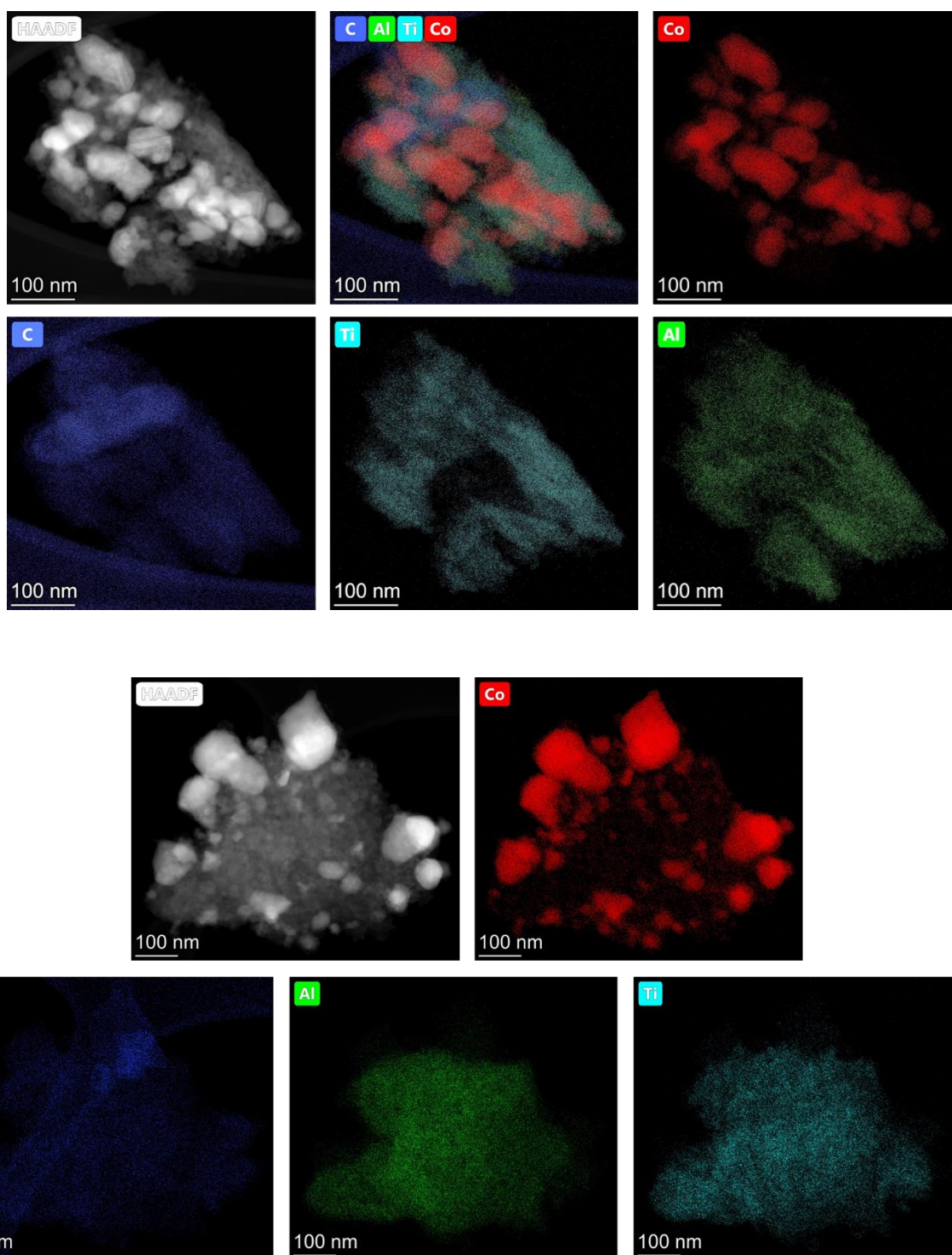


Figure S16. HAADF-STEM images of $\text{Co}_3\text{O}_4/\text{Ti}_2\text{AlC}$ catalyst after stability test at $650\text{ }^\circ\text{C}$.

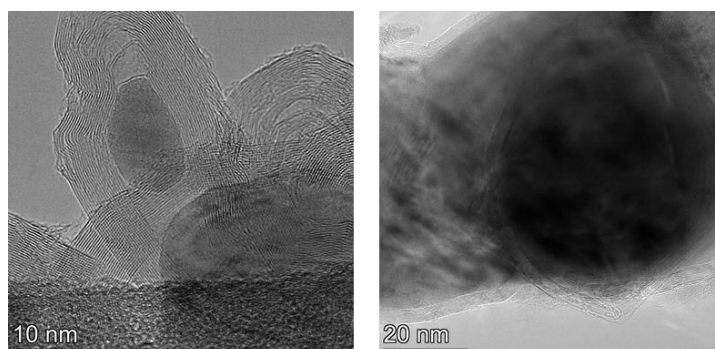


Figure S17. TEM images of $\text{Co}_3\text{O}_4/\text{Ti}_2\text{AlC}$ catalyst after stability test at 650 °C, showing the formation of carbon nanotubes covering some Co_3O_4 particles.